Journal of Low Temperature Physics, Vol. 68, Nos. 3/4, 1987

Effects on DC SQUID Characteristics of Damping of Input Coil Resonances

Jukka Knuutila and Antti Ahonen

Low Temperature Laboratory, Helsinki University of Technology, Espoo, Finland

Claudia Tesche

IBM Thomas J. Watson Research Center, Yorktown Heights, New York

(Received January 23, 1987)

The possibility of improving dc SQUID performance by damping the input circuit resonances caused by parasitic capacitances is studied experimentally. A high-quality dc SQUID was coupled to a first-order axial gradiometer built for neuromagnetic research, and a resistor–capacitor shunt was connected in parallel with the input coil of the SQUID. Ten different RC *shunts were studied with the SQUID operating in a flux-locked loop, carefully shielded against external disturbances. It was found that increasing the shunt resistance resulted in smoother flux–voltage characteristics and smaller noise. At best, the minimum obtainable equivalent flux noise level was one-fourth that for the unshunted SQUID. The noise level is a function of the shunt resistance* R_s *only, except for shunt capacitance values bringing the low-frequency resonance of the input coil close to the flux modulation frequency. At a constant bias current level, where the amplitude of the flux–voltage characteristics is at maximum, the equivalent flux noise varies as* $R_s^{-0.7}$*. The results agree reasonably well with recently published predictions based on numerical simulations where the whole input circuit with parasitic capacitances was taken into account.*

1. INTRODUCTION

The advent of modern, high-quality, thin-film dc SQUIDs offering at least an order of magnitude better flux sensitivity than rf SQUIDs[1] has started a new era in the construction of very sensitive magnetometers to be used, e.g., in neuromagnetic studies.[2,3] However, the closely coupled input coils of SQUIDs necessary for practical devices introduce several new

0022-2291/87/0800-0269$05.00/0

problems not present in autonomous SQUIDs. The most prominent feature is the extra capacitance across the SQUID loop. This parasitic capacitance, studied by several authors with simulations[4-8] and experiments,[9-12] gives rise to resonances in the SQUID loop and hysteresis in the current-voltage characteristics accompanied by excess noise. The input coil and the SQUID loop also form a transmission line whose $\lambda/2$ resonances often fall near the points of operation.

The noise level of SQUIDs suffering from the capacitance effects depends very strongly on the flux bias point in the SQUID ring. Thus, it may be possible to operate a SQUID in the small-signal mode with carefully chosen flux bias at noise levels even comparable to those theoretically obtainable with autonomous SQUIDs.[13,14] However, any attempts to use a practical configuration with flux modulation and phase-locked loop have resulted in a substantially deteriorated energy resolution.[11,15-17]

Besides the parasitic capacitances caused by the input coil, the loading of the SQUID by an external input circuit can have a significant effect on its performance.[9,15,18-21] Also, flux transformers are always accompanied with parasitic capacitances, which may form a resonant circuit with a very high Q.

Recently, it has been pointed out by Seppä and Ryhänen[8] on the basis of numerical simulations with the complete input circuit and parasitic elements taken into account that these resonances may give rise to excess noise in the SQUID output. This happens although the resonances are normally located at much lower frequencies than the Josephson oscillations at ordinary working points. Damping of these resonances might result in reduced noise and smoother SQUID characteristics. This can be accomplished, without the introduction of low-frequency noise, by connecting a series combination of a resistor and a capacitor across the input coil.

Practical SQUID magnetometers often have to be operated in environments where there is a substantial amount of rf interference. Thus, some sort of input filtering is almost always desirable, since the SQUID operation is very easily degraded in the presence of spurious fields. The introduction of an RC shunt across the input coil also provides an effective rf filter; normally its passband is below a few MHz.

In this work, the changes in the dc SQUID voltage-flux characteristics and in the noise level caused by damping the external input circuit resonances by means of different RC shunts are studied experimentally. As an application, the results obtained here have been used in optimizing the dc SQUID performance of a seven-channel, high-sensitivity magnetometer[22,23] for neuromagnetic studies. The device has been constructed in the Low Temperature Laboratory of Helsinki University of Technology, and it employs IBM thin-film dc SQUIDs.[24]

2. *RC* SHUNT CHARACTERISTICS

A lumped circuit model for the flux transformer input circuit with a parasitic capacitance C_p and a damping shunt (R_s and C_s) is shown in Fig. 1a. This is equivalent to the circuit of Fig. 1b, where

$$R'(\omega) = \frac{1}{(1+\alpha)^2 + (\omega\alpha\tau_s)^2} R_s \tag{1}$$

$$C'(\omega) = \frac{(1+\alpha)^2 + (\omega\alpha\tau_s)^2}{1+\alpha+\omega^2\tau_s^2\alpha} C_s \tag{2}$$

Here, the parameter $\alpha = C_p/C_s$, the time constant $\tau_s = R_s C_s$, and the angular frequency $\omega = 2\pi f$. For simplicity, the losses in R_p associated with the parasitic capacitance C_p have been neglected. This can be justified in the usual practical case where $R_p \ll R_s$ and $C_s > C_p$.

The resonant frequency of this circuit is given by

$$\omega_R^2 = \frac{\tau_s^2\alpha - L'C_s(1+\alpha)^2 \pm \{[L'C_s(1+\alpha)^2 - \tau_s^2\alpha]^2 + 4(1+\alpha)L'C_s\tau_s^2\alpha^2\}^{1/2}}{2L'C_s\tau_s^2\alpha^2} \tag{3}$$

For small α this is well approximated by

$$\omega_R^2 = \left[1 - \left(1 - \frac{\tau_s^2}{L'C_s}\right)\alpha\right] \frac{1}{L'C_s} \tag{4}$$

where $L' = L_p L_i/(L_p + L_i)$, L_p and L_i being the inductances of the pickup and input coils, respectively. In most cases ω_R is only very weakly dependent on R_s. The Q value of the lumped circuit model is

$$Q = \frac{1+\alpha+\omega_R^2\tau_s^2\alpha}{\omega_R\tau_s} \tag{5}$$

When the coupling to the SQUID is taken into account, the input coil inductance must be replaced by an effective value. As a small-signal approximation, the circulating current J in the SQUID is modeled as

$$J = -\Phi/\mathscr{L} = -MI_i/\mathscr{L} \tag{6}$$

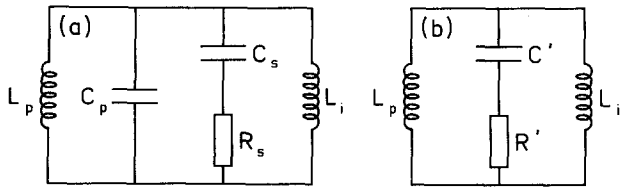

Fig. 1. (a) The flux transformer circuit with parasitic capacitance and an *RC* shunt. (b) Equivalent circuit.

where M is the mutual inductance between the SQUID and the input coil, I_i is the current through the input coil, and $\mathscr{L}$ is the effective dynamic input inductance of the SQUID. The effective input coil inductance is then

$$L_i^{\text{eff}} = L_i(1 - k^2 L_s/\mathscr{L}) \tag{7}$$

where k is the coupling constant and L_s is the geometrical inductance of the SQUID.

Theoretical calculations[4] and measurements of the input impedance of the SQUID[9] indicate that the effective input coil inductance at the normal flux-locked-loop operating points of the SQUID is reduced by 10–20%, thus leading only to relatively small corrections in the resonant frequency and to the Q value of the input circuit.

At high frequencies, the imaginary part of the effective input impedance of the SQUID, defined as $j\omega\mathscr{L}^{-1} = \mathscr{L}^{-1} + j\omega\mathscr{R}^{-1}$, where $\mathscr{R}$ is the dynamic input resistance, should also be taken into account.[9] However, for the IBM SQUID, near 10 MHz and below, this component is negligible.

The flux Φ_a applied to the SQUID is given as a function of frequency by

$$\Phi_a = M\Phi_e H(j\omega)/(L_i + L_p) \tag{8}$$

where Φ_e is the external flux applied to the pickup coil L_p and $H(j\omega)$ is the frequency-dependent flux transfer function

$$H(j\omega) = \left(1 - \frac{\omega^2 L'C'(\omega)}{1 + j\omega R'(\omega)C'(\omega)}\right)^{-1} \tag{9}$$

The power spectrum of the noise current through the input coil L_i caused by Johnson noise from the resistor R_s is given by

$$S_i(\omega) = \frac{\omega^2 C_s^2 L_p^2}{(L_i + L_p)^2\{[1 - \omega^2 L'(C_s + C_p)]^2 + \omega^2 R_s^2 C_s^2(1 - \omega^2 L'C_p)\}} S_e^R \tag{10}$$

with $S_e^R = 4k_B T R_s$. The energy of the resistor noise is concentrated near the resonance frequency, and at low enough frequencies its contribution is negligible. Again, in Eqs. (8)–(10) the effect of the SQUID on the input circuit is taken into account by using an effective input inductance, Eq. (7).

Although $S_i(\omega)$ is small at low frequencies, part of the high-frequency noise may be seen at low ω in the output of the readout system because of mixing-down effects. This contribution can be estimated using small-signal Fourier analysis.

If the SQUID is operated in the flux-locked mode, using square-wave flux modulation, the voltage over the SQUID in response to a small signal flux Φ_s is proportional to $\Phi_s U(t, \omega_M)$, where $U(t, \omega_M)$ is a square wave of frequency $f_M = \omega_M/2\pi$ and of unit amplitude. The flux-locked loop keeps

the operating point of the SQUID constant. Assuming that the transfer function of the impedance matching network and the preamplifier is $G_t(\omega)$ and that the detecting consists in multiplying the preamplifier output by $U(t, \omega_M)$, one has for the Fourier transform of the voltage $V_0(t)$ at the output of the detector

$$\tilde{V}_0(\omega) \propto \{G_t(\omega)[\tilde{\Phi}_s(\omega) * \tilde{U}(\omega, \omega_M)]\} * \tilde{U}(\omega, \omega_M) \tag{11}$$

where the tilde denotes the Fourier transform and $*$ the convolution integral. Assuming now that $G_t(\omega)$ is nonzero only near ω_M and that the input signal is white noise whose spectral components are totally uncorrelated, one has for the amplitude spectrum of the detector output at frequencies ω much less than ω_M

$$|\tilde{V}_0(\omega)| = A\left[\tilde{\Phi}_s(\omega)^2 + \sum_{m=1}^{\infty} \frac{2}{(4m^2-1)^2} \tilde{\Phi}_s(2m\omega_M)^2\right]^{1/2} \tag{12}$$

where A is a constant.

The low-frequency output given by Eq. (12) consists of the direct term $\Phi_s(\omega)$ and of the terms due to mixed-down resistor noise near even harmonics of the modulation signal. In practice the summation index m in Eq. (12) has a cutoff because the bandwidth of the flux modulation signal extends only up to a few MHz; also, the coefficients of the mixed-down terms decay very rapidly as a function of m. From the relative amplitudes of the mixing terms with respect to the direct term it is thus easy to get an estimate for the contribution of the resistor in the output noise.

It has to be noted that if the transfer function of the impedance matching circuit and the preamplifier is independent of frequency and if the flux modulation and the detector reference signals are perfect square waves, all the mixing terms resulting from Eq. (11) cancel, leaving only the direct term $\Phi_s(\omega)$.

3. MEASUREMENTS

Our experiments were carried out with one IBM dc SQUID[24] connected to an axial, first-order, asymmetric gradiometer wound of 0.2-mm-diameter Nb wire on a ceramic glass former. The SQUID and the gradiometer coil parameters are shown in Tables I and II, respectively.

The voltage–flux characteristics and equivalent flux noise levels of the flux-locked SQUID at various bias points were recorded for the unshunted case and for the ten different R_sC_s combinations, which are listed in Table III together with the calculated resonance frequencies and Q values as given by Eqs. (3) and (5). The table also shows the estimated noise contributions of the shunt resistor in flux units, as calculated by the method described

TABLE I

SQUID Parameters

Critical current	$I_c = 40\ \mu A$
Resistance	$R_{nn} = 1.4\ \Omega$
Stewart-McCumber parameter	$\beta_C = 0.07$
Inductance parameter (input coil open)	$\beta_L = 1.9$
Input coil inductance	$L_i = 0.7\ \mu H$
Coupling coefficient	$k = 0.9$

TABLE II

Gradiometer Coil Parameters

Pickup coil diameter	$d_{pu} = 20.0$ mm
Pickup coil height	$h_{pu} = 7.0$ mm
Number of turns in pickup coil	$n_{pu} = 6$
Compensation coil diameter	$d_c = 24.5$ mm
Compensation coil height	$h_c = 15.0$ mm
Number of turns in compensation coil	$n_c = 4$
Total inductance (including connection leads)	$L_p = 1.44\ \mu H$
Field at pickup coil producing 1 Φ_0 into the SQUID	320 pT

in the previous section and for 74-kHz flux modulation signal with harmonics extending up to 3 MHz. The assumed input inductance $\mathscr{L}$ of the SQUID for Eq. (7) was $5L_s$, where L_s is the geometrical inductance of the SQUID loop. This gives an effective input coil inductance of $0.8L_i$. As an example, the calculated transfer function (9) and spectral density of the noise current (10) are shown in Fig. 2 as functions of frequency for one shunt.

TABLE III

The *RC* Shunts Studied, along with Their Resonance Frequencies, *Q* Values, and Estimated Noise Contributions

R_s, Ω	C_s, nF	f_{res}, MHz	Q	$\Phi_n, 10^{-6}\Phi_0/\sqrt{\text{Hz}}$
0.1	470	0.36	10	3.2
0.1	22	1.7	44	0.5
0.1	0.68	9.2	270	<0.1
0.5	470	0.36	1.9	4.9
0.5	22	1.7	8.8	0.5
0.5	0.68	9.2	53	<0.1
3.3	470	0.36	0.3	4.0
3.3	22	1.7	1.3	0.6
3.3	0.68	9.2	8.1	<0.1
14.7	0.68	9.2	1.8	<0.1

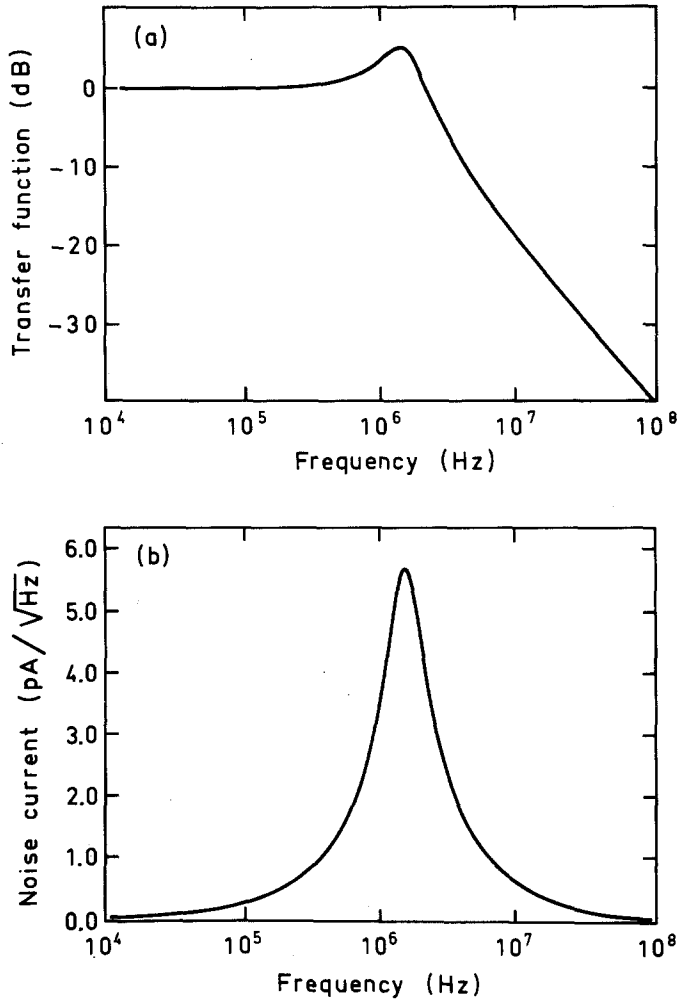

Fig. 2. (a) The transfer function $H(j\omega)$, Eq. (9), and (b) the spectral density of the noise current $S_i^{1/2}$ due to Johnson noise in the shunt resistor through L_i for $R_s = 3.3\ \Omega$ and $C_s = 0.68$ nF, as given by Eq. (10).

All the measurements were carried out inside our magnetically shielded room[25] with the SQUID and the pickup coil surrounded by a superconducting shield of 47 mm inner diameter. The SQUID electronics, except for the preamplifier, was in a separate rf-shielded cabinet outside of the shielded room, and all the cable feedthroughs were carefully filtered to ensure the absence of external rf interference.

The SQUID was connected via an impedance matching resonant transformer to a tuned preamplifier of an equivalent noise temperature less than 2 K.[22] The operating frequency was 74 kHz and the harmonics of the square-wave modulation signal extended to roughly 3 MHz. The flux-voltage characteristics were recorded using square wave flux modulation, which switched between a constant value and a level swept over several flux quanta by means of a 100-Hz sawtooth signal.

In all our noise measurements the SQUID was operated in the flux-locked loop with a peak-to-peak modulation of $\Phi_0/2$. The noise spectra were measured with an HP 3561A spectrum analyzer. The white noise levels were obtained by measuring the rms value of the output voltage over a 40-Hz bandwidth from an average of 25 spectra, extending from zero to 100 Hz, and dividing by the square root of the bandwidth. The standard deviation of this estimate[26,27] is about 1%. To get the result in flux units, the spectral density of the voltage was then divided by the separately measured change of the output voltage corresponding to a flux quantum.

4. RESULTS AND DISCUSSION

In Fig. 3 the flux-voltage characteristics in the unshunted case and with five shunts are shown. The curves are recorded at $I_{\text{bias}} = 47\ \mu\text{A}$, where the amplitude is at maximum. It is noted that the characteristics tend to be smoother with increased damping. In the unshunted case there is even a reversal in the gain $\partial V/\partial\Phi$. The systematic change in the behavior is seen more clearly in Fig. 4, where the V-Φ characteristics are shown as functions of bias current for the unshunted SQUID and for the same SQUID with two different shunts. The undamped SQUID (Fig. 4a) must be biased very high up to achieve smooth operation. This is in agreement with the results of the double-loop analysis, where a family of double-valued solutions exist for low bias currents.[4] The damped SQUID can be operated at lower bias where the gain is higher. In addition, the maximum amplitude of the V-Φ characteristics is higher than in the unshunted case and stays approximately at the constant level of 30 μV. Note also that for the highly damped SQUID (see Fig. 4c) the curves are smooth everywhere, but the gain at high bias is very small. A similar smoothening of the V-Φ characteristics was observed by de Waal *et al.*,[15] who measured the voltage-flux characteristics of their dc SQUID with the input coil open and shunted with a 1-kΩ resistor.

Examples of noise spectra recorded in 100- and 10-Hz bandwidths are shown in Fig. 5. The noise is white down to well below 1 Hz. In Fig. 6a the minimum noise level obtained is shown as a function of the shunt resistor and capacitor values. For the unshunted case, the minimum noise level was $16.3 \times 10^{-6}\Phi_0/\sqrt{\text{Hz}}$. From Fig. 6a it is seen that the minimum noise level

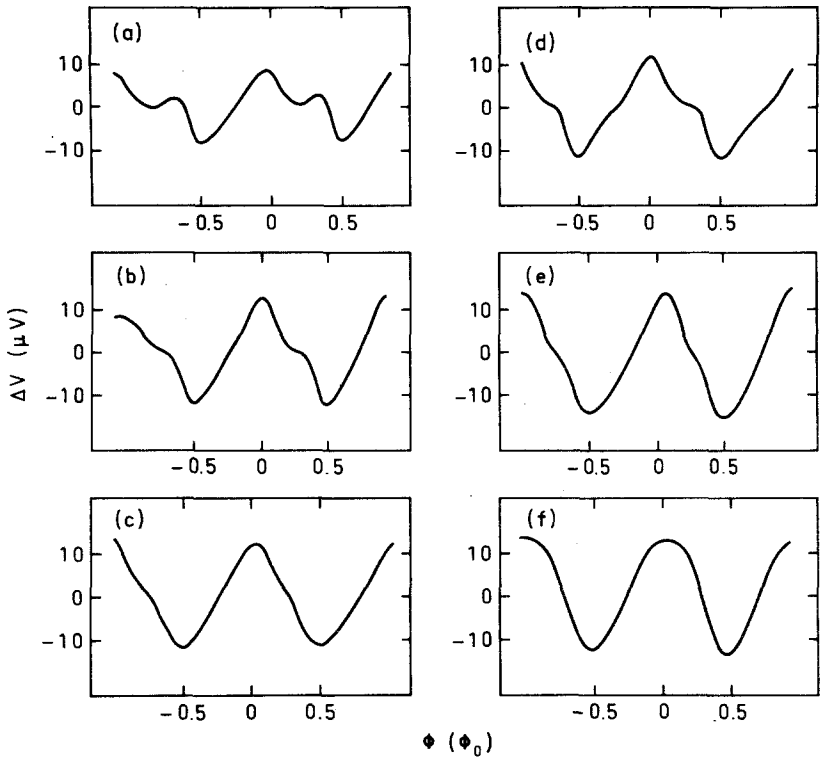

Fig. 3. The ac component of the voltage-flux characteristics at bias current $I_{bias} = 47\ \mu A$. (a) No shunt, (b) $R_s = 0.1\ \Omega$, $C_s = 22$ nF, (c) $R_s = 0.5\ \Omega$, $C_s = 22$ nF, (d) $R_s = 0.5\ \Omega$, $C_s = 0.68$ nF, (e) $R_s = 3.3\ \Omega$, $C_s = 22$ nF, (f) $R_s = 14.7\ \Omega$, $C_s = 0.68$ nF.

tends to decrease with increasing shunt resistance, being four times less than the unshunted level for $R_s = 14.7\ \Omega$ and $C_s = 0.68$ nF. Due to reasons to be discussed later, consistently higher noise was observed in the case of shunts having $C_s = 470$ nF than with $C_s = 22$ and 0.68 nF. For the latter group, the noise level is a decreasing function of R_s, independent of the capacitor value.

As seen from Table III, the estimated contributions due to the resistor thermal noise are significantly smaller than the measured levels. Thus, the observed dependence on R_s cannot be explained only by the thermal noise of the resistor itself.

In the simulations of Seppä and Ryhänen[8] the presence of the input coil resonance is clearly seen in the SQUID output voltage distribution: thermal-noise-induced switching from the running solution to the zero-voltage state traps the system to metastable beating solutions, locked to the

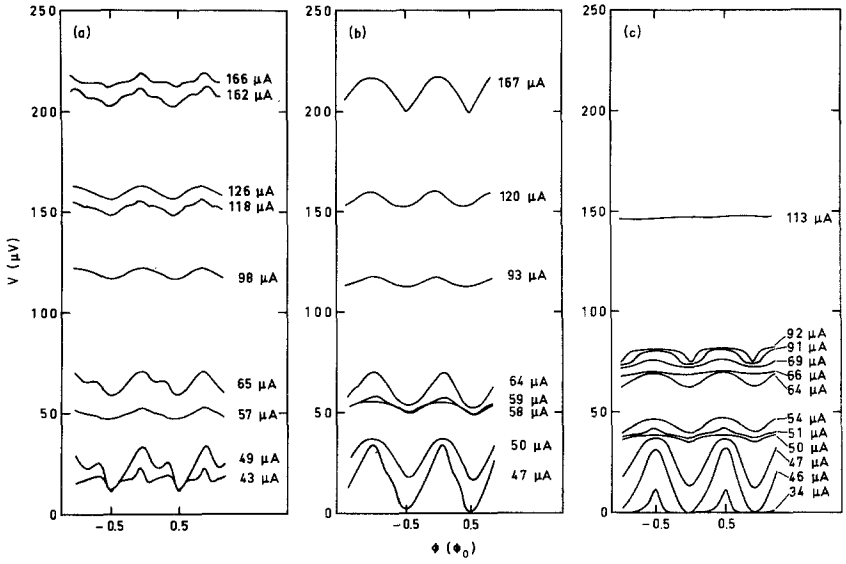

Fig. 4. The voltage-flux characteristics as a function of bias current. (a) No shunt, (b) $R_s = 3.3\ \Omega$, $C_s = 22$ nF, (c) $R_s = 14.7\ \Omega$, $C_s = 0.68$ nF.

resonances of the signal coil. Increased damping decreases hopping between different states. These transitions are also seen in the current-voltage characteristics.

The switching between solutions introduces excess noise in the output, also seen in the numerical simulations. Generally, for a two-level system of lifetimes τ_0 and τ_1, with $\tau_1 \ll \tau_0$, the spectral density of the excess noise at frequencies much less than τ_1^{-1} is proportional to τ_1.[28] Here, τ_1 is the lifetime of the resonant beating state, which can be approximated by its Q value Q_R divided by the angular resonance frequency. For $C_s \gg C_p$,

$$\tau_1 \simeq Q_R/\omega_R \simeq L'/R_s + C_p R_s \tag{13}$$

In our experiments with fixed inductances one would, on the basis of Eq. (13), expect the noise first to decrease with increasing R_s, independent of C_s. When R_s becomes larger than $(L'/C_p)^{1/2}$ the noise level should rise again and approach the level of the unshunted SQUID because the damping by R_s becomes ineffective. In our case, this critical value of R_s is of the order of 100 Ω. Thus, all the experiments considered here were done in the $1/R_s$ region.

In Fig. 6a the dependence of the noise level on the inverse of R_s is rather weak, varying as $R_s^{-0.15}$. One has to remember, however, that all the points in this plot were obtained by optimizing the bias current for best

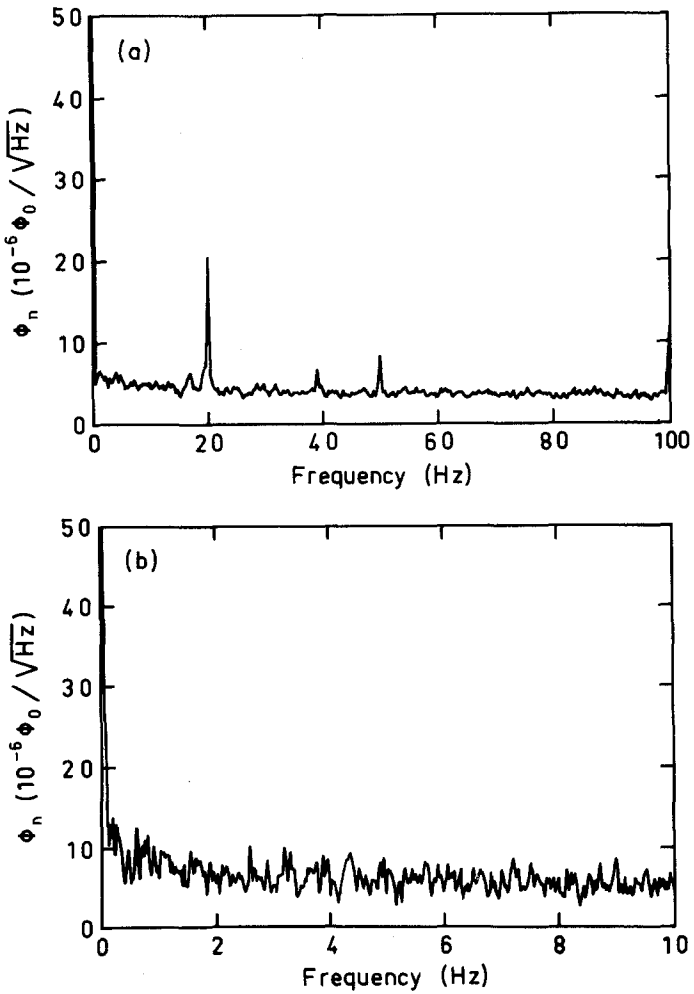

Fig. 5. Noise spectra for $R_s = 14.7\ \Omega$ and $C_s = 0.68$ nF at $I_{bias} = 47\ \mu$A, for (a) 100-Hz bandwidth, (b) 10-Hz bandwidth. The extra peaks are due to power line interference and mechanical resonances.

performance separately in each case. In Fig. 6b the noise levels are shown at constant bias ($I_{bias} = 47\ \mu$A); the effect is now seen more clearly, the noise level being proportional to $R_s^{-0.7}$.

The differences in the R_s dependences in Figs. 6a and 6b are partly attributable to the behavior of the optimum bias point. With higher damping the bias point where the noise level is at a minimum shifts lower toward the point where the amplitude of the V-Φ curve is at a maximum. This is

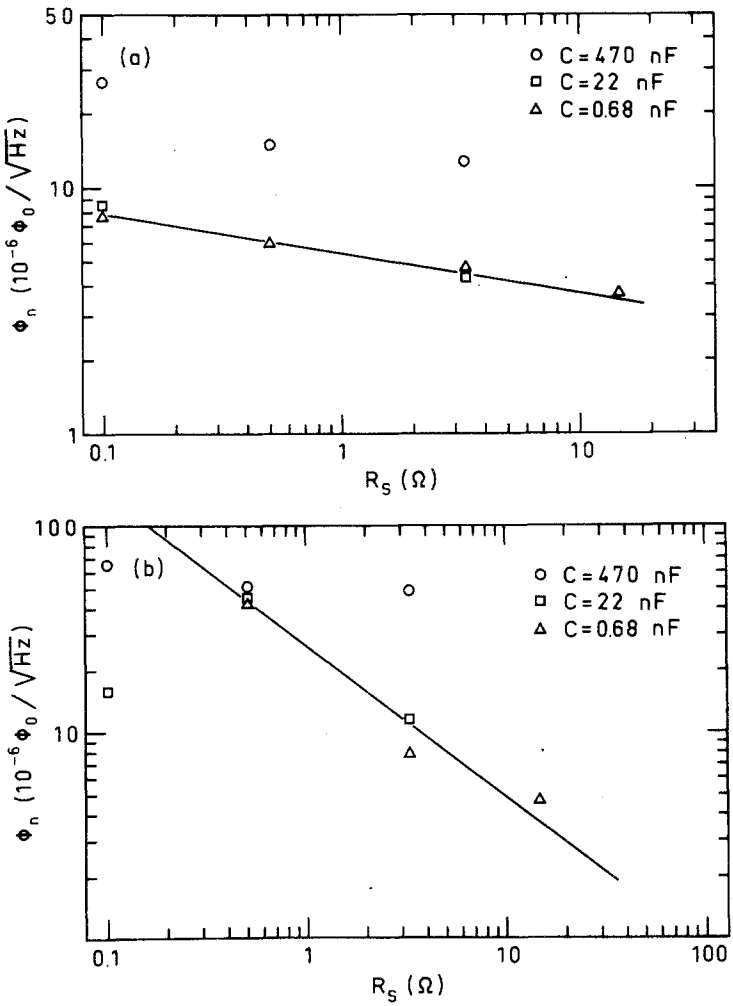

Fig. 6. (a) Minimum equivalent flux noise level obtained versus shunt resistance R_s for different values of the shunt capacitance C_s; the bias current was optimized separately for each shunt; (b) noise levels at fixed bias current $I_{bias} = 47\ \mu A$.

demonstrated in Fig. 7, where the noise level versus bias current is shown for the undamped SQUID and for two shunts.

The change in the noise level as a function of R_s at higher bias currents, for example, near 100 μA, is not as prominent as near the critical current of the SQUID. There are at least two mechanisms contributing to this. First, at low bias currents the probability of the excursions from the running solution toward the zero-voltage solution is greater than at higher bias

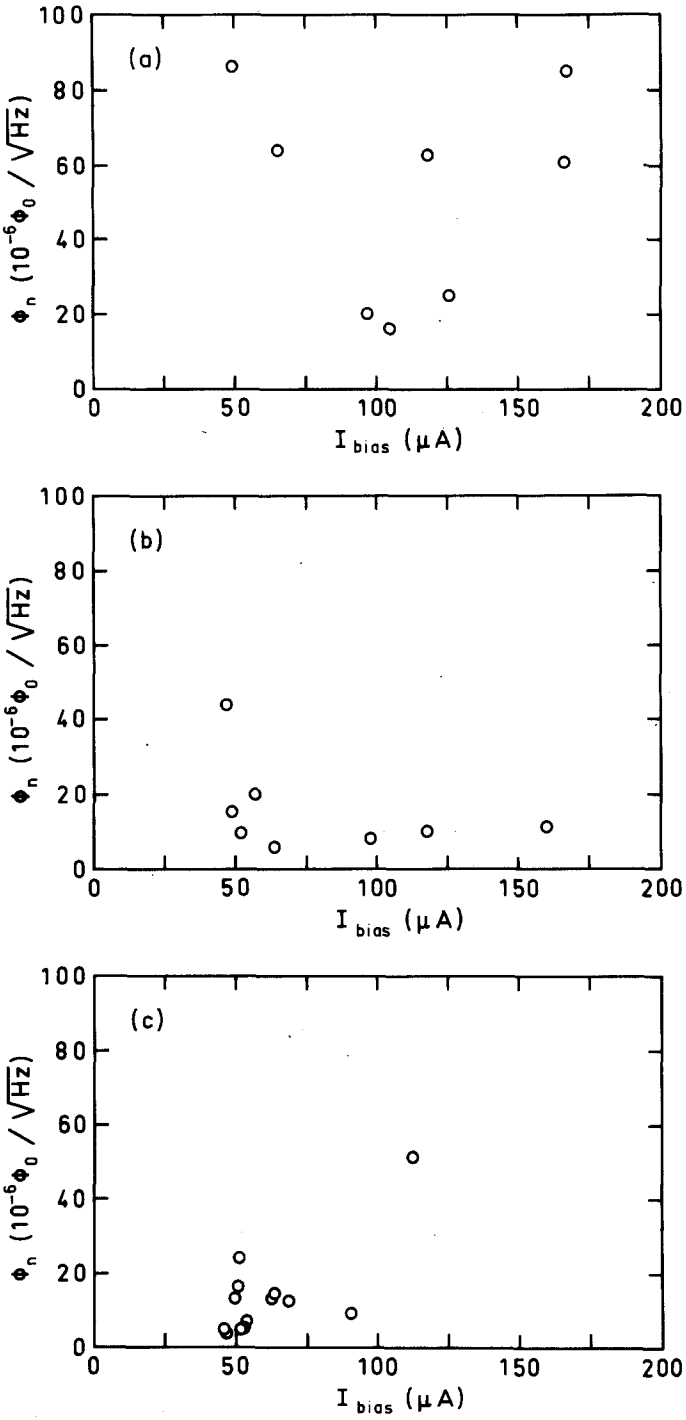

Fig. 7. Equivalent flux noise as a function of bias current. (a) No shunt, (b) $R_s = 0.5\,\Omega$, $C_s = 22$ nF, (c) $R_s = 14.7\,\Omega$, $C_s = 0.68$ nF.

currents, thus augmenting the effect of switching noise. Second, at high bias and thus at very high operating frequencies the magnetic coupling between the SQUID and the input coil is weakened because the wavelengths of the Josephson oscillations become smaller than the total length of the input coil. Therefore, at high bias the SQUID with an input coil behaves more like an autonomous SQUID. This is also consistent with the observations of Hilbert and Clarke.[9]

In all cases of RC shunts with $C_s = 470$ nF considerably higher values of output noise were measured. The behavior is probably due to strong interference of the input circuit with the square wave signal used in flux modulation. The input circuit resonance frequency with these shunts, 360 kHz, is very near the fifth harmonic of the flux modulation square wave signal, resulting in an enhanced fifth harmonic and damped higher harmonics in the actual modulating flux. The large ripple in the flux modulation signal caused by the shunt forces the flux bias point to move around and to spend more time in low-gain and thus high-noise regions. The interference with the carrier signal is also seen in recording the V-Φ characteristics using the technique described above: with large modulation amplitudes covering several flux quanta the signal decreases markedly because of averaging caused by the ripple. In proper square wave modulation the flux bias is most of the time at two distinct operating points with low equivalent flux noise and high gain and the transitions through higher noise (low-gain) regions are fast.

5. CONCLUSIONS

The experimental comparison of an IBM dc SQUID with the computer simulations by Seppä and Ryhänen[8] presented here is, of course, only qualitative. The exact theoretical description of the system is very difficult; a model that takes into account the parasitic elements in the SQUID and in the signal coil is, as the authors point out, very massive to be simulated numerically. A second point is that it is almost impossible to predict the actual coupling between the SQUID and the input coil, because at very high frequencies the SQUID becomes decoupled. It is very likely that the amount of coupling drastically affects the behavior of the SQUID-flux transformer combination.

The results described here also have some practical implications. As discussed above, proper damping of signal coil resonances favors relatively high R_s. To keep the noise level due to this resistor within acceptable limits, it is necessary to keep the resonant frequency of this damped circuit well above the operating frequency. The noise energy of the resistor is then spread over a large interval of frequency, having no sharp peaks and

negligible spectral density below the carrier frequency. The relatively high resonant frequency is also important for avoiding interference with the flux modulation signal.

The required minimum value of the resonance frequency may, however, conflict with the demand of input filtering in most practical magnetometers. Often there is a substantial amount of rf noise relatively close to the operating frequency caused, for example, by near-by radio stations. For best performance, the input shunt should be optimized with respect to both proper damping and input filtering. Of course, one has to remember that rf interference may wipe out the SQUID operation completely, whereas the optimum resonance damping is only fine-tuning, since the improvement of the noise level with increased damping tends to be the smaller, the more damping there is.

In conclusion, we have shown that damping of the resonances in the input circuit can smooth the characteristics of a given SQUID and reduce the noise considerably, even though the resonant frequency is well below the Josephson frequencies. In designing an input filter to reduce rf interference, this aspect should also be taken into account, preferably by testing the actual configuration with different damping combinations.

ACKNOWLEDGMENTS

The authors wish to thank Heikki Seppä for many stimulating and clarifying discussions, Olli V. Lounasmaa and Matti Kajola for comments and suggestions, Jari Hällström and Istvan Derka for building the dc SQUID electronics, and Jim Rozen and Robert Sandstrom for their assistance in bonding and packaging the SQUID.

REFERENCES

1. J. Clarke, *Physica* **126B**, 441 (1984).
2. R. Hari and R. J. Ilmoniemi, *CRC Crit. Rev. Biomed. Eng.* **14**(2), 93 (1986).
3. S. J. Williamson and L. Kaufman, *J. Magn. Magn. Mater.* **22**, 129 (1981).
4. C. D. Tesche, *J. Low Temp. Phys.* **47**, 385 (1982).
5. M. Gershenson, R. Hastings, R. Schneider, M. Sweeny, and E. Sorensen, *IEEE Trans. Magn.* **MAG-19**, 2058 (1983).
6. K. Enpuku, K. Sueoka, K. Yoshida, and F. Irie, *J. Appl Phys.* **57**(5), 1691 (1985).
7. D. Drung and W. Jutzi, in *SQUID'85—Superconducting Quantum Interference Devices and Their Applications*, H. D. Hahlbohm and H. Lübbig, eds. (de Gruyter, Berlin, 1985), p. 807.
8. H. Seppä and T. Ryhänen, in Proceedings of the 1986 Applied Superconductivity Conference, *IEEE Trans. Magn.*, submitted for publication (1987).
9. C. Hilbert and J. Clarke, *J. Low Temp. Phys.* **61**, 237 (1985).
10. P. Carelli and V. Foglietti, *IEEE Trans. Magn.* **MAG-19**, 299 (1983).
11. P. Carelli and V. Foglietti, *IEEE Trans. Magn.* **MAG-21**, 424 (1985).
12. B. Muhlfelder, J. A. Beall, M. W. Cromar, R. H. Ono, and W. W. Johnson, *IEEE Trans. Magn.* **MAG-21**, 427 (1985).

13. C. D. Tesche and J. Clarke, *J. Low Temp. Phys.* **29**, 301 (1977).
14. V. J. de Waal, P. Schrijner, and R. Llurba, *J. Low Temp. Phys.* **54**, 215 (1984).
15. V. J. de Waal, T. M. Klapwijk, and P. van den Hamer, *J. Low Temp. Phys.* **53**, 287 (1983).
16. C. M. Pegrum, D. Hutson, G. B. Donaldson, and A. Tugwell, *IEEE Trans. Magn.* **MAG-21**, 1036 (1985).
17. B. Muhlfelder, J. A. Beall, M. W. Cromar, and R. H. Ono, *Appl. Phys. Lett.* **49**(17), 1118 (1986).
18. R. S. Germain, M. L. Roukes, M. R. Freeman, R. C. Richardson, and M. B. Ketchen, in *Proceedings of the 17th International Conference on Low Temperature Physics LT*-17, U. Eckern, A. Schmid, W. Weber, and H. Wühl, eds. (Elsevier, Amsterdam, 1984), p. 203.
19. C. D. Tesche, *Appl. Phys. Lett.* **41**(5), 490 (1982).
20. C. D. Tesche, *IEEE Trans. Magn.* **MAG-19**, 458 (1983).
21. J. M. Martinis and J. Clarke, *J. Low Temp. Phys.* **61**, 227 (1985).
22. A. I. Ahonen, J. K. Hällström, M. J. Kajola, J. E. Knuutila, C. D. Tesche, and V. A. Vilkman, in *Proceedings of the 11th International Cryogenic Engineering Conference ICEC11*, G. Klipping and I. Klipping, eds. (Butterworth, Guildford, 1986), p. 820.
23. J. Knuutila, A. Ahonen, J. Hällström, M. Kajola, O. V. Lounasmaa, V. Vilkman, and C. Tesche, to be published (1987).
24. C. D. Tesche, K. H. Brown, A. C. Callegari, M. M. Chen, J. H. Greiner, H. C. Jones, M. B. Ketchen, K. K. Kim, A. W. Kleinsasser, H. A. Notarys, G. Proto, R. H. Wang, and T. Yogi, *IEEE Trans. Magn.* **MAG-21**, 1032 (1985).
25. V. O. Kelhä, J. M. Pukki, R. S. Peltonen, A. A. Penttinen, R. J. Ilmoniemi, and J. J. Heino, *IEEE Trans. Magn.* **MAG-18**, 260 (1982).
26. P. D. Welch, *IEEE Trans. Audio Electroacoust.* **AU-15**, 70 (1967).
27. J. S. Bendat and A. G. Piersol, *Random Data: Analysis and Measurement Procedures* (Wiley, New York, 1971), Chapter 9.6.
28. M. R. Beasley, D. D'Humieres, and B. A. Huberman, *Phys. Rev. Lett.* **50**, 1328 (1983).